Aerothermal theory of easily penetrable roughnes: Particular application to the atmospheric flow in and over longscale spray cooling system(*)

YE. A. GAYEV(**)

Candidate of Physical-Mathematical Science, Senior Scientific Researcher
Institute of Hydromechanics, Ukrainian National Academy of Sciences
Zhelyabov str., 8/4, 252057, Kiev, Ukraine.

Summary. — An extended spray cooling system (SCS) for powerful thermal or nuclear electric station has been treated as a kind of artificial, industrial landscape; its interaction with atmosphere is of great interest both for industrial and environment protection purposes. The theoretical model of SCSs follows after the results of field measurements of aerothermal wind transformation caused by SCS. The model takes into consideration the main features of SCS such as deceleration of the air flow within the drop layer, and saturation of the air flow with heat and water vapour. Other examples of *penetrable roughness* have been discussed and this concept has been proposed as the hydromechanic base linking different relevant disciplines. Other literature has been reviewed in this framework.

PACS 92.60.Fm – Boundary layer structure and processes.
PACS 47.15 – Laminar flows.
PACS 01.30.Cc – Conference proceedings.

1. – Introduction

Artificial, industrial landscapes are frequently met on our planet today. Extended *spray cooling systems* (SCS) are a particular kind of such landscapes. To know how they interact with atmospheric wind is necessary both for project designers and for their current engineering exploitation. On the other hand, there is strong influence of wasted heat and moisture from the SCS on the immediate atmosphere. Therefore, such an artificial complex terrain in the near atmospheric layer should be considered also from the environment protection point of view.

(*) Paper presented at EUROMECH Colloquium 338 "Atmospheric Turbulence and Dispersion in Complex Terrain" and ERCOFTAC Workshop "Data on Turbulence and Dispersion in Complex Atmospheric Flows", Bologna, 4-7 September 1995.
(**) E-mail: gayev@gayev.pp.kiev.ua

There are numerous other technical and geophysical applications where there is surface layer filled with some obstacles in the bottom part of the flow, with some important physical or biophysical processes taking place within it. It means that the flow inside this layer is of especial great interest for researchers. In spite of the fact that the physical nature of such structures in the flow may essentially differ, due to which they are studied by specialized independent disciplines, we propose the general point of view, the concept of *penetrable roughness* which allows to elaborate the hydromechanical theory able to extrapolate results obtained in one discipline to another one and to give the rules and criteria of similarity and laboratory modelling.

2. – Longscale spray cooling systems. Field investigation of Ladizhin SCS

To obtain effective heat dissipation in circular water supply systems, spray coolers have been for a long time widely used for thermal and nuclear power electric plants especially in the USA and in countries of the former USSR. Up-to-date spray cooling systems (SCS) give an example of human-made artificial terrains that are formed by a number of tall fountains. Getting a big output of warm water from power plant, fountains divide it into plenty of drops, sized from several microns to 6–10 mm, thus ensuring developed heat and mass exchange surface. In this way, the SCSs provide the cooling of water $\Delta t = 7 \div 10°$ C for summer conditions if its initial temperature is $30 \div 42°$ C. Although the droplets are small, their concentration n within drop layer $x > 0, \ 0 \leq z \leq h$ is high enough and reaches 2000–300 000 drops$/\mathrm{m}^3$ depending on their radii and level of considered space point. Extended spray cooler is shown to have sufficient influence on the environment and should be investigated both for industrial purposes and for prevention of unfavorable influence on the near atmosphere.

For instance, Ladizhin thermal power plant SCS (Middle Ukraine; generating capacity 1800 MW, came into commission in 1972) is an open channel 1000 m long and 90 m wide with 1300 fountains with height $h = 6$ m placed over the channel and having total water output 21 m$^3/$s.

Zaporozh'ye nuclear power plant SCS (South Ukraine; its construction began in 1985 and now it has a capacity of 6000 MW) is arranged as two parallel open channels 1500 m long and 90 m wide containing 21 spraying modules of $300\,\mathrm{m} \times 90\,\mathrm{m}$ size with total water output $105\,\mathrm{m}^3/$s.

So the problem of interaction between SCS and atmosphere is important.

For the last 30 years the experience in exploitation of extended spray cooling systems in different meteorological conditions has been accumulated. It is clear now that the functioning of spray coolers is connected with a great number of physical phenomena. It was found out that the dependence of SCS operations on meteorological conditions or on design parameters is different from the dependence of a single fountain or even a small spray basin. It is explained by wind deceleration and air saturation with vapour while the wind is moving along the system. Thus, the first part of this paper is devoted to the mechanism of interaction of the atmosphere and the artificial terrain in the form of extended drop layer.

The mechanism of spray cooling system functioning was not highlighted. Only American researchers [1] made attempts to estimate the decrease of SCS cooling efficiency in the direction along the wind. We have managed to perform a more detailed SCS study on a large thermal power electric station nearby the town of Ladizhin (middle Ukraine) in summers 1981 and 1982 [2].
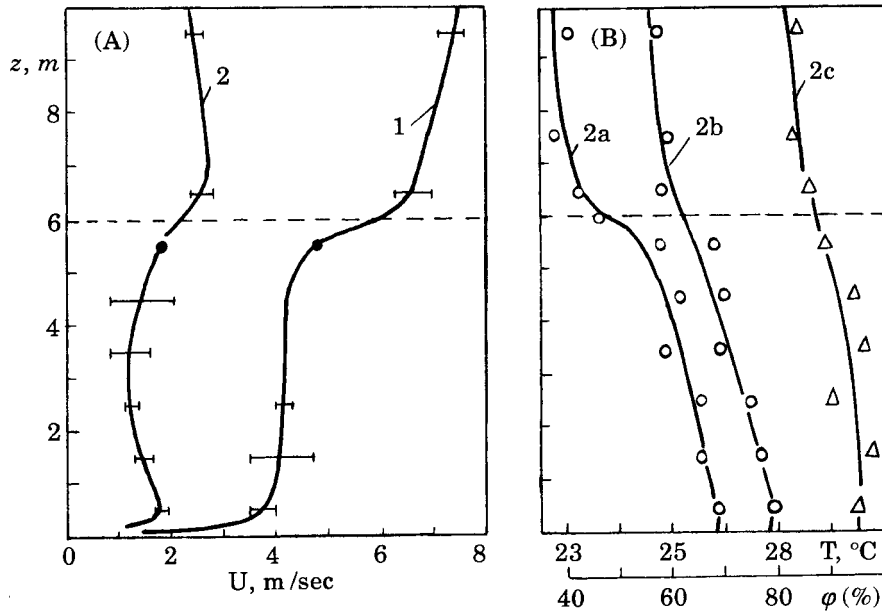
Fig. 1. – Typical distributions of wind velocity (A) and aerothermal characteristics (B) inside spray cooling system (*i.e.* below the dashed line $z = h = 6$ m) and above it; 1: measurement No. 5, afternoon August 1, 1980, strong wind; 2: measurement No. 6, evening August 1, 1980, weak wind. (Curves 2a and 2b: temperatures on wet and dry thermometers; 2c: calculated relative humidity.)

A floating gradient mast was placed inside the SCS and had ten cup-anemometers and ten special aspiration psychrometers at different levels z and a wind vane at the top of the mast. Six of the measuring device pairs were placed within the droplet layer, and four of them were located over it in the free wind stream. Horizontal roofs shielded the devices from the sprayed drops. Anemometers and dry and wet temperature-sensitive resistors of the psychrometers were also remotely monitored, so that the registration equipment was connected with them by cable and placed in a special floating cabin 20 m downwind. Measuring devices were calibrated in laboratory before the field work and after it.

The profiles of the average wind velocity $U(z)$, temperatures on dry $T(z)$ and wet $T_{w}(z)$ thermometers both inside the droplet layer, $0 \leq z \leq h$, and over it up to 10 m height were obtained in 12 test series. Some results, not published yet, can be seen in fig. 1. Relative humidity $\varphi(z)$ was defined according to the standard psychrometric table. More data may be found in our papers [2–4] published mainly in Russian.

Note that the profile distributions are quite different from those over smooth surface. Two parts of the profiles have to be discussed. Over the top SCSs level, $z = h = 6$ m, the wind velocity distributions grow monotonically in case of strong wind; the temperature diminishes as a rule. Some cases where the wind velocity diminishes over the SCS are characterized by weak external wind so that the horizontal forced convection is perhaps comparable with intensive natural convective motion rising up from heated and wetted air layer within SCS.

Inside the drop layer, the wind velocity profiles have distortions similar to those which are observed in plant canopies, [5,6]. The profiles inside the drop layer are likely to reflect

the work of the drops as sinks of kinetic energy and sources of heat and humidity.

One can conclude that the horizontal air output through the layer $0 \leq z \leq h$ considerably decreases and depends on drop concentration. It is necessary to know this air discharge, if we want to make all aerothermal estimations correctly. The humidity inside SCS is very high. Therefore, subsequent torches cool water worse than the previous ones.

Non-monotonic velocity profiles having their extremum on lower levels of a drop layer seem surprising. But they are not a mistake in the measurement. The theory given below makes it possible to explain this phenomenon. The extremum on the velocity profile is caused by non-homogeneity of drop concentration $n(z)$ and the effect of drop drift with the air flow.

3. – More examples of penetrable roughness

The drop layer over storming ocean resembles the situation described above. In this situation it has been established that the droplets have a significant influence on the wind and moisture profiles [7].

Forest or other vegetation canopies is another example of penetrable structure under the atmospheric wind. Meteorologists investigate air motion through such canopies as well as heat and gas exchange in them to predict the microclimate in canopies, their influence on the near atmosphere, protection capacity of green belts, growth of agricultural production and so on. Meteorologists have been studying this subject for 40 years. Extensive reviews can be found in [5, 6, 8].

Mean wind distributions in a forest and over it, studied in [3, 5, 6], show that the main feature of the wind distribution within the plant canopy is its distortion. The profiles of wind velocity are evidently rather similar to those in SCS. The cause is easy to understand: leaves, stems and branches play the role of obstacles for the wind decelerating it. The leaves work also as sources of heat, of water vapour and of O_2 and CO_2 gases. Vertical distributions of these parameters within the vegetation canopy can be found out in specialized literature.

Some measured wind profiles show also "bulges" or "secondary maximums" on them inside the vegetation layer. This phenomenon is explained by canopy morphology, *i.e.* vertical non-uniformity of the canopy. (A similar phenomenon inside the drop layer mentioned above should require one more mechanism to be explained.)

A rather unexpected example of the PR is a "canopy layer within an infinite cluster of wind turbines" [9]. Clusters of closely packed buildings, an industrial or a residential area, become nowadays a priority object of discussion in wind engineering [10].

So, the nature of obstacles in the layer $0 \leq z \leq h$ proved to be not very important. The idea arises to simulate such clusters by means of an arbitrary permeable layer, for example, made of nets or rods. Some simple patterns in the form of numerous rows of overflowed obstacles situated over a smooth surface were studied experimentally in the wind channel by the thermoanemometric technique [3]. The results highlight the organized vortex layout behind the individual obstacles. There were big vortices behind the obstacles in the form of a flat equilateral triangle with side lengths of 30 mm that cross one another. And intensive turbulence was relatively homogeneous and of small scale when the obstacles were taken in the form of rods $d = 2\,\mathrm{mm}$ in diameter, $h = 70\,\mathrm{mm}$ in height, with the distance 15 mm ($\sim 7.5d$) between them. Some mean velocity profiles can also be seen in [3].

Developed roughness is frequently used for heat exchangers for controlling and enhancing heat dissipation. In hydrology, the resistance factor or sediment transport flow

capacity of channels having flexible vegetation or artificial roughness are studied [11].

Structures similar to those described above play the role of roughness for the external flow. On the other hand, they are permeable for the flow, and just the motion through them and physical processes inside them (mechanical motion of roughness elements, heat and mass exchange, etc.) are of primary interest for research and practice. So, the idea of *penetrable roughness* (PR) seems to represent their most common properties and may serve as the basis for theoretical treatment.

4. – Mathematical modelling of easily penetrable roughness

Due to obstacles in the flow, a number of individual forces and sources of contaminants

$$F = \frac{1}{2}\rho c_x (U - u)^k S, \qquad I_T = \alpha(T - t)S_0, \qquad I_E = \beta(E - e)S_0,$$

act in roughness layer. Generally speaking, the horizontal speed of obstacles (drops) u, their temperature t and the saturating vapour concentration close to their surfaces $e = a_0 t + a_1$ depend on the coordinates x, z and on drop size as well. (We use capital symbols for air flow, and the small ones for obstacles.)

Let us restrict ourselves to the case of additive source properties, when the bulk mass force, or contaminant source intensity is the sum of all the single forces, or intensities acting in the unit volume Ω:

(1) $$f = \lim \frac{\sum F_i}{\rho\Omega}, \qquad i_T = \lim \frac{\sum I_{iT}}{\rho\Omega}, \qquad \text{while } \Omega \to 0.$$

This case occurs if the distance between obstacles is about 5-7 times or more their dimension, so that the vortices behind them do not interact strongly. Having this hypothesis in mind, let us call such kind of PR an *easily penetrable roughness, EPR*.

The Prandtl's boundary layer approach seems to be valid both in free and in decelerated flow parts provided the forced horizontal convection dominates. Within the PR layer, $z \in [0, h]$, the equations of the flow motion, heat and mass transfer in it should contain some source terms. Besides, equations for the "own life of the PR elements" should be taken into consideration. It can be written in the most generalized form

(2)
$$\begin{cases} \rho_1\left(U\dfrac{\partial U}{\partial x} + V\dfrac{\partial U}{\partial z}\right) = \dfrac{\partial \tau}{\partial z} - \dfrac{1}{2}c_x\rho_1\displaystyle\int_0^\infty (U - u)^k S(r)n(r)\mathrm{d}r, \\[2ex] \dfrac{\partial U}{\partial x} + \dfrac{\partial V}{\partial z} = 0, \\[2ex] m(r)\left\{u(r)\dfrac{\partial u}{\partial x} - v(r)\dfrac{\partial u}{\partial z}\right\} = \dfrac{1}{2}c_x\rho_1\{U - u(r)\}^k S_0, \\[2ex] \rho_1 c_1\left(U\dfrac{\partial T}{\partial x} + V\dfrac{\partial T}{\partial z}\right) = \dfrac{\partial j_T}{\partial z} + \alpha\displaystyle\int_0^\infty (T - t)S_0(r)n(r)\mathrm{d}r, \\[2ex] \rho_1\left(U\dfrac{\partial E}{\partial x} + V\dfrac{\partial E}{\partial z}\right) = \dfrac{\partial j_E}{\partial z} + \beta\displaystyle\int_0^\infty (E - e)S_0(r)n(r)\mathrm{d}r, \\[2ex] mc_2\left\{u(r)\dfrac{\partial t}{\partial x} - v(r)\dfrac{\partial t}{\partial z}\right\} = \alpha\{t(r) - T\}S_0(r) + \beta\mathcal{L}\{e(r) - E\}S_0(r). \end{cases}$$

The free air flow outside the EPR, over it, behaves according to an equation system like (2) in which all the source terms as well as the 3rd and 6th equations are omitted, *i.e.* according to the common boundary layer equation system. It is evident that the flows over and within the EPR, and the physical processes in them, are to be matched by the conjugation (coupling) conditions on their separating level besides the common boundary conditions [4, 12]:

$$
(3) \qquad U\mid_{z=h-0} = U\mid_{h+0}, \qquad V\mid_{h-0} = V\mid_{h+0}, \qquad \tau\mid_{h-0} = \tau\mid_{h+0},
$$

$$
T\mid_{z=h-0} = T\mid_{h+0}, \qquad j_T\mid_{h-0} = j_T\mid_{h+0}, \qquad E\mid_{h-0} = E\mid_{h+0}, \qquad j_E\mid_{h-0} = j_E\mid_{h+0}.
$$

A consequence of sub-models follows from the general model (2), (3). Let us discuss them explaining, if required, some symbols used above.

1. *EPR made up of immobile particles* is the easiest possible sub-model, [4, 12] which is obtained from (2), (3) if assuming $\partial n/\partial r = 0$ and $u(z) \equiv 0$. Such a model simulates plant canopies in the atmospheric flow and is an appropriate tool for investigation of the air flow retardance. Even this particular model makes it possible to explain the real variety of velocity distributions in forests and possible extremum on them caused by vertical non-homogenity of obstacle concentration $n(z)$. A numerical analysis has been published in [4, 12].

2. *EPR made up of monodisperse drifted particles*, the second model, explains phenomena in the drop layer. It is assumed that obstacles (simulating drops of given radius r) can be drifted by the carrying flow with some horizontal velocity $u(z)$. Therefore, in addition to the prediction of wind profile transformation, the new model also predicts drop entrainment into air motion. Processes of heat exchange and drop evaporation are the most significant ones for this model and can be predicted numerically [4]. Droplets are treated as a continuous medium there.

3. *The full model of multi-disperse drop layer.* Generally, real obstacles, or drops, are known to be of wide spectrum of sizes. For this reason we consider the frontal and full surface drop area S and S_0, the drop mass m, and especially the drop concentration $n(z; r)$ to depend on the radius r. So we deal with a number of drop media characterized by $u(r), t(r), e(r)$. If the radius r runs discrete values from r_1, $r_2, \dots$ to r_K, then sums must replace integrals in the source terms and both the 3rd and the 6th equation are equal to K equations corresponding to every r_K. The corresponding results will be considered in detail here.

5. – Properties of flow formed by the EPR

Most of the following results were obtained by numerical computation by some finite-difference approximation method [13].

Let us assume for simplicity that there are drops of three radii only. Then we substitute integrals by sums and the 3rd and 6th equations by three equations each in the equation system (2). Figure 2 represents the velocity field transformation both for air and drop media in several consequent cross-sections of the EPR; the non-dimensional distance $\overline{x}$ along the drop layer has been used here according to formula (5). One can note that the strongest perturbation takes place in the *initial region* $0 \leq x \leq l$ of the EPR; the initial region length $l = l(n, r, U_\infty, \dots)$ could be calculated according to this theory. Vertical velocity distributions are complex, but the division of the flow into internal and external parts proposed here helps analyze them.
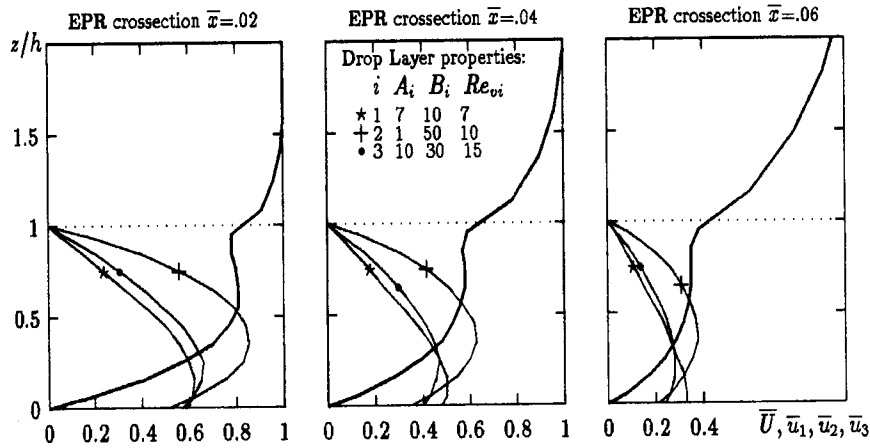
Fig. 2. – Wind profiles and speed distributions of drops of 3 kinds along the EPR.

Within the EPR the horizontal speed of wind and that of the drops decrease sharply along it. Shear stress $\tau = \rho\nu_T(z)\frac{\partial U}{\partial z}$ can be neglected in comparison with the drag-induced force (1) acting here, so that if we imagine an impenetrable film between the internal and external flows, *i.e.* on the level $z = h$, the motion within EPR would stop after passing the initial region. But the role of τ increases along the droplet layer, and finally an equilibrium between f and τ occurs. Since the shear stress supplies kinetic energy into the retarded flow part from the free one and in this way supports the motion in it (as well as heat and mass exchange), then the vertical distributions of velocity become stable and no longer change their shape. We call this part of the obstacle layer, which extends theoretically till infinity, the *main region*([1]). Bearing in mind such properties of both regions, one may arrive at two more simple systems with ordinary derivatives instead of the equation system (2) with partial derivatives. Under certain conditions they can be solved analytically and supply us with convenient estimations of important parameters, [4, 12, 13]. These results are used in our summarized analysis.

Wind profiles within the initial region of the uniform EPR, *i.e.* $n(z) = \mathrm{const}$, increase monotonically. They become non-monotonic for a non-uniform structure of the EPR, if $\mathrm{d}n/\mathrm{d}z \neq 0$. Such phenomenon known for the "immobile particle model" is called "the secondary maximum" or "the bulge phenomenon" by meteorologists [6]; it reflects the morphology of vegetation layer. The "bulge" disappears in the main region of the EPR.

The situation is more complex for the droplet layer, *i.e.* for the "driftable particles" model. Droplets are supposed to be regularly generated on the upper EPR level $z = h$ and then to fall down at the given vertical speed component $v(z;r)$. Therefore, their concentration turns out to be a function of the vertical coordinate z:

$$n = \frac{\dot{N}}{v(z;r)}, \quad 1/\mathrm{m}^3.$$

Theoretically we may assume $v(z)$ to be constant and obtain that $n \equiv \mathrm{const}$. However, the "bulges" on the velocity profiles do not disappear, see fig. 2, as it would have been in a

---

([1]) This and the above definitions correspond to the definitions "Impact region" and "Array interior" of [10].

uniform forest. This result also confirms the surprising wind profiles obtained in our field experiments. The following explanation can be given. The horizontal speed of drops is yet rather small at the top EPR levels but it almost approaches the speed of the local wind on the middle levels. Since the distributed force (1) depends upon the difference $U - u$, it is higher on the top levels, $f_{\text{top}} > f_{\text{middle}}$, causing stronger air deceleration there than on the middle levels. This secondary maximum disappears in the main region where the drag force is counteracted by the shear stress.

Speed distributions for each kind of drops are presented in fig. 2 under numbers 1, 2, 3. Naturally, they are also transformed along the EPR. It is also necessary to comment on the form of these profiles. While the drops are moving in the fast air flow from the top to the middle levels, they increase their speed taking away kinetic energy from the flow and accumulating it. After the drops have reached the local wind speed (in the point where curves $u_i(z)$ intersect the curve $U(z)$, see fig. 2), they continue to fall down and u is now higher than $U(z)$, since $U(z)$ goes to 0 at the wall. This results in drop deceleration and therefore one can see the maximum on drop velocity profiles. Besides, the accumulated kinetic energy returns back to the wind flow and speeds it up a little, depending on the mass of the drops. Such kind of wind-droplet energy exchange first discovered by observations over the stormy ocean surface was called "non-turbulent" exchange mechanism [7].

Engineers prefer to deal with monodisperse drop layer. So, the problem of a "mean" drop size arises. In the work [14] some estimations for the "mean" dimensionless parameters have been deduced.

If n, the concentration of obstacles within the EPR, is high enough, the stagnation of the air flow may appear in the bottom EPR levels [4, 12, 13]. Portions of the kinetic energy no longer penetrate to the bottom surface, now they penetrate only to some "depth of penetration" l_{p}. Such a "non-blowing phenomenon" often observed in forests is purposely used in the green belts. Power engineers should avoid such situations causing stagnation of the heat and mass exchange. The function $l_{\text{p}} = l_{\text{p}}(n, U_\infty, ...)$ could be estimated analytically [12].

Processes of heat and mass exchange form a microclimate inside and round the spray coolers. Let us consider these processes for some "equivalent" monodisperse EPR, fig. 3. The curve sets (I) and (II) show that the dimensionless air temperature $\overline{T}(z)$ and vapour concentration (humidity) $\overline{E}(z)$ increase while the air is moving along the EPR and getting heat and water vapour from the obstacles (drops). Heated and moistened boundary layer develops above and along the EPR in the wind direction Ox. All the drops are supposed to have the same dimensionless temperature $\overline{t} = \overline{t}(x, h) = 1$ on the top $z = h$. Vertical distribution of their temperature $\overline{t}(z)$ has a complex shape being transformed from one cross-section towards another (curves (III)). Since the air becomes more and more warm and wet, the drop cooling $\Delta(x) = \overline{t}(x, h) - \overline{t}(x, 0)$ gradually decreases along the EPR. The deepest drop cooling takes place in the front cross-section $x = 0$ where the drop temperature profile, which has been found to have the form

$$(4) \qquad t_0(z) = t(0, z) = \frac{\pi_0 + \pi_1}{\pi_1} \exp\left[a\pi_1(1 - z)\right] - \frac{\pi_0}{\pi_1},$$

is taken as initial boundary condition.

Similar to hydrodynamic properties, there is an *initial* and *main thermal region* in the flow picture. Along the second one, there is an equilibrium between the replenishment of heat and vapour from the cooling and evaporating drops and the removal of these substances into the external fresh flow. Ordinary derivative equations following from (2) may be used to estimate the length of the initial thermal region as well as the depth zone of
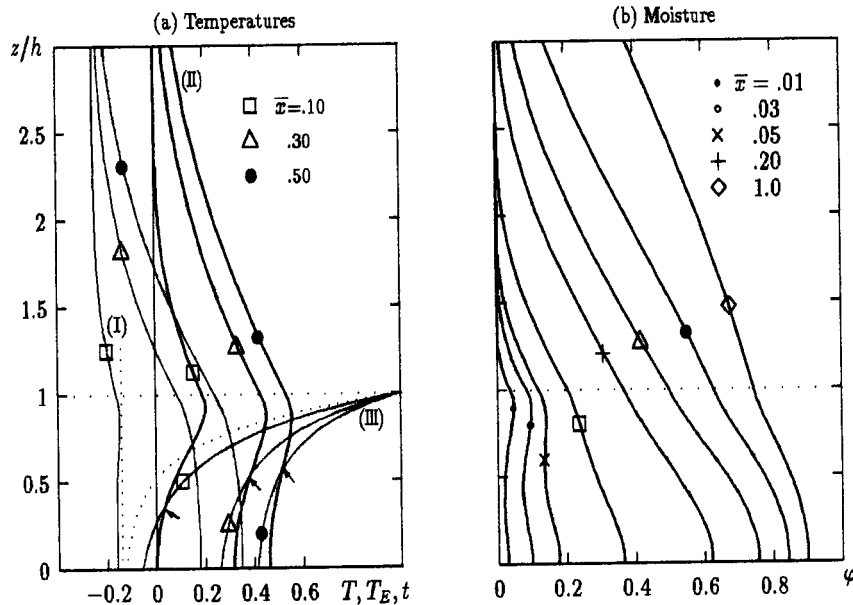
Fig. 3. – a) Humidity (I), as well as main flow temperature (II) and drop temperature (III) distributions; b) relative moisture distributions along EPR in the form of drop layer.

possible thermal stagnation, the limit shape of $T(z)$ and $E(z)$ within the main aerothermal region [13].

We use "formal temperature" $T_E = (E - a_1)/a_0$ instead of E to make three temperature curves in fig. 3 comparable. Naturally, the drop temperature $t(z)$ is attracted to the $T(z)$ as well as to the $T_E(z)$ while drops are falling down. Due to it, the curves $t(z)$ start to cross the corresponding curves $T(z)$ (in the points shown by short arrows) so that the drop temperature turns out to be lower than the air temperature, $t < T$, on EPR levels below this point. It means that the heat exchange changes its direction to the opposite one, the air starts to reheat the drops and is cooled by them (note "bulges" on the curves $T(z)$ along all the main region). Comparison of flux distributions j_T and j_E draws attention to the fact that the processes of heat and mass exchange are not analogous within EPR [13].

Let us imagine that the drops continue their fall down below the water surface $z = 0$. Three curves $T(z)$, $t(z)$ and $T_E(z)$ would reach their common local value called the "wet bulb temperature" T_M in meteorology and in theory of coolers. It varies along the EPR, $T_M = T_M(x)$, and its initial value is found from (4):

$$T_M = -\frac{a_1 B_E}{a_0 B_E + B_T}.$$

A quotient of local humidity at some space point to the saturated humidity $E_* = e(T)$

$$\varphi = \frac{E}{E_*}$$

characterizes relative humidity of the local surroundings. The distribution of this

aerothermal parameter inside and above the drop layer is shown in fig. 3b). In the numerical example under consideration, the humidity is never more than 100% but in a real large spray cooler φ is close to 100% in most part of it.

If in some space point it proves to be $T_E \geq T$, it means that the air humidity $E = e(T)$ is more than the saturated humidity E_*, and therefore vapour condensation and formation of dew drops are possible here. The temperature T_E formally introduced above now acquires the meaning of "the point of dew". This phenomenon is out of consideration in this paper.

Wishing to link studies *in situ* with both laboratory simulation and theory, modern science requirement is to conduct researches in non-dimensional form. That's why we endeavoured to find the most convenient dimensionless variables and parameters to be used here. A satisfying solution for the exponent $k = 2$ in the system (2) has not been found yet. The linear case of $k = 1$ is much easier for research.

About 15 physical quantities govern the situation in the model (2). We recommend the following non-dimensional variables:

$$\overline{x} = \frac{1}{Re}\frac{x}{h}, \qquad \overline{z} = \frac{z}{h}, \qquad \overline{U} = \frac{U}{U_\infty}, \qquad \overline{V} = Re\frac{V}{U_\infty},$$

(5)

$$\overline{T} = \frac{T - T_\infty}{t_h - T_\infty}, \qquad \overline{E} = \frac{E - E_\infty}{e_h - E_\infty}, \qquad \overline{t} = \frac{t - T_\infty}{t_h - T_\infty}, \qquad \overline{e} = \frac{e - E_\infty}{e_h - E_\infty}.$$

Then, only nine dimensionless criteria fully describe this kind of EPR:

$$A = \frac{SnU_\infty h}{\nu}, \qquad A_T = \frac{\alpha n h^2 S_0}{\rho_1 c_1 \nu}, \qquad A_E = \frac{\beta n h^2 S_0}{\nu},$$

$$B = \frac{c_x}{2}\frac{\rho_1 S h^2 U_\infty}{m\nu}, \qquad B_T = \frac{\alpha h^2 S_0}{\nu m c_2}, \qquad B_E = \frac{b\beta\mathcal{L}h^2 S_0}{\nu m c_2},$$

$$Pr = \frac{\nu}{\lambda/\rho_1 c_1}, \qquad Sc = \frac{\nu}{D}, \qquad \sigma = -\frac{vr}{\nu}.$$

Their number can be reduced for the initial or the main region. It can be stated that the pair $\{\frac{U}{U_h(x)}, \frac{z}{h}\}$ can be viewed as universal variables for the internal flow, and the pair $\{\frac{U-U_h}{U_*}, \frac{z-h}{d(x)-h}\}$ as that for the external flow.

Corresponding results were implemented into spray cooling system design of Zaporozh'ye nuclear power plant [4]. It was supposed earlier that the smaller the drops, the higher the cooling capacity, and this is the matter of fact for a single spray. Contrary to this conclusion, the present theory discovers that the cooling efficiency of a large spraying system depends only to a small extent on the drop size d, since penetration of drop layer decreases, and this is as d^{-3}.

6. – Turbulence within the EPR

Special attention should be paid to the turbulence regime modeling within the penetrable roughness. Turbulent regime is known to be formed by interaction of vortices

behind obstacles. We proposed a generalization of the Prandtl's mixing-length hypotheses since the mean characteristics of the flow field were of major interest to us.

Fluxes of momentum, heat and mass are taken in their common gradient form,

$$\tau = \rho\nu_T\frac{\partial U}{\partial z}, \qquad j_T = \rho\lambda_T\frac{\partial T}{\partial z}, \qquad j_E = \rho D_T\frac{\partial E}{\partial z}.$$

Exchange coefficients are considered to be approximately constant within EPR but follow Prandtl's hypotheses over it:

$$\lambda_T/c_1 = D_T = \nu_T = \begin{cases} \nu_{T_0}, & z \in [0, h], \\ l^2\frac{\partial U}{\partial z}, & l = l_h + \kappa(z - h), \quad z \geq 1. \end{cases}$$

The above method of conjugation

$$\nu_T|_{z=h-0} = \nu_T|_{z=h+0}$$

is applied again to get the matching mixing length l_h. The "logarithmic" profiles

$$U = U_h + U_*C_1(Ri)\ln\left(1 + \frac{z-h}{z_0}\right), \qquad T = T_h + T_*C_2(Ri)\ln\left(1 + \frac{z-h}{z_0}\right), \qquad E = ...,$$

$$z_0 = l_h/\kappa, \qquad C_1 = C_2 = 1/\kappa, \text{ if } Ri = 0$$

which can be deduced under the approximation $\tau = \text{const}$, $j_T = \text{const}$, ... for $z \geq h$, are more convenient than those with a "displacement height" parameter [5, 6].

The degree of atmospheric instability is especially high over spray coolers. The formula of Monin-Obuchov reflects this influence by adding a linear term to the usual logarithmic profiles [6]. We take another course and use an empirical relationship $C_i = C_1(Ri)$ [15].

7. – Conclusion. Further problems

We tried to prove that the concept of easily penetrable roughness supply reflects the predominant physical processes of its interaction with the atmospheric flow. The question is now whether the theory can be adopted for investigation of further important features of real penetrable structures met in the nature and in human practice.

Thus, the real structure of the drop layer formed by an industrial SCS is much more complex then it is treated above. The methodological model [16] shows the way to cover the variation of the initial drop speeds and of the motion of the drop first upward (from the nozzle level to the spray top) and then downward (to the water surface). Other phenomena, like fog and dew creation, solar radiation absorption, are on to-day's agenda both for industrial and environment protection aims.

Every kind of permeable structure in the flow "lives" its own "life". The problem is how to include such peculiarities in the unified theory. A "waving phenomenon" is characteristic for vegetation canopies. Equations used by meteorologists can be treated as advanced equations of the mechanical state of the EPR made up of immobile obstacles.

One of the tasks of the urban engineering is to predict air flow vorticity and turbulent flow statistics between buildings within residential or industrial area. Contrary to the "easily" PR, the wakes behind such obstacles are much longer and therefore interact with

one another much more intensively. One should speak of "roughness penetrable with difficulty" that can be described by the above given model if the force term and the source term (1) include coefficients reflecting such interaction and known from hydromechanics. Thus, "equations of the state of PR" seem to be just the appropriate way to extend the theory for new structures.

One shortcoming of the above theory is important to be mentioned. It always gives the "secondary maximums" on initial region only, while experiments of meteorologists in forests discover them also for very long fetches, [6]. This is recent topic of discussions in their discipline, which means that models of turbulence must be greatly improved. It implies, of course, this theory too.

This Colloquium as well as the Conference "Flow and Dispersion Through Groups of Obstacles" held in 1994 at Cambridge stresses the tendency to master an overall approach. One of the possible ways has been proposed by us here.

* * *

I am indebted to the European Research Community of Flow, Turbulence and Combustion (ERCOFTAC) that sponsored the presentation of this material to EUROMECH Colloquium 338 and ERCOFTAC Workshop (Bologna, September 4-7, 1995). I would like to express also my gratitude to Prof. F. TAMPIERI (FISBAT-CNR, Italy) for his interest in my work. Discussions and mutual work with Dr. E. SAVORY (Surrey University, UK) also helped me in generalizing these ideas.

REFERENCES

[1] CHATURVEDI S. and PORTER R. W., *Trans. ASME, J. Fluid Engin.*, **100** (1978) 65-72.
[2] GAYEV YE. A., TSIMBAL V. S. and NICKITIN I. K., *The Works of the Ukrainian Meteorological Institute*, **216** (1986), pp. 69-75 (in Russian).
[3] GAYEV YE. A., MELENEVSKY V. V., NICKITIN I. K. *et al.*, in *Mechanica neodnorodnikh i turbulentnikh techenij*, edited by V. V. STRUMINSKY (Nauka, Moscow) 1989, pp. 107-115 (in Russian).
[4] GAYEV YE. A., in *Proc. 9th Cooling Tower and Spraying Pond Symposium*, (Rhode-Saint-Genese, Belgium) 1994.
[5] DUBOV A. S., BICKOVA L. P. and MARRUNITCH S. V., *Turbulence in a Vegetation Canopy*, (Hydrometeoizdat, Leningrad) 1978 (in Russian).
[6] RAUPACH M. R. and THOM A. S., *Annu. Rev. Fluid Mech.*, **13** (1981) 97-129.
[7] BORTKOVSKY R. S., *Heat and vapour exchange between the atmosphere and ocean during storm* (Hydrometeoizdat, Leningrad) 1983 (in Russian).
[8] GAYEV YE. A., in *Berichte des Bioklimatologischen Instituts in Göttingen*, 1996 (to be published).
[9] EMEIS S. and FRANDSEN S., *Boundary Layer Meteorol.*, **64** (1993) 297-305.
[10] JERRAM N., PERKINS R. J., FUNG J. C. H., DAVIDSON M. J., BELCHER S. E. and HUNT J. C. R., in *Wind Climate in Cities. NATO Advanced Study Institute* (Karlsruhe, July 1993).
[11] KOUWEN N., UNNY F. E. and HILL H. M., *J. Irrigation and Drainage Div, Proc. ASCE* 95, No. IR2 (1969), pp. 329-342.
[12] GAYEV YE. A., *Fluid Mech. - Sov. Res. (USA)*, **19** (1990) 1.
[13] GAYEV YE. A., *Annual Report 1995* (Institute of Hydromechanics, Ukrainian National Academy of Sciences) 1996.
[14] GAYEV YE. A. and SABAYEVA L. M., *Fluid Mech. - Sov. Res. (USA)*, **19** (1990) 13.
[15] NICKITIN I. K., *Complex turbulent flows and processes of heat and mass exchange* (Naukova dumka, Kiev) 1980 (in Russian).
[16] GAYEV YE. A., *Hydromechanicka*, **66** (1993) 33 (in Russian).